Spatiotemporal dynamics of calcium signals during neutrophil cluster formation

Roxana Khazen[a], Béatrice Corre[a], Zacarias Garcia[a], Fabrice Lemaître[a], Sophie Bachellier-Bassi[b], Christophe d'Enfert[b], and Philippe Bousso[a,1]

Neutrophils form cellular clusters or swarms in response to injury or pathogen intrusion. Yet, intracellular signaling events favoring this coordinated response remain to be fully characterized. Here, we show that calcium signals play a critical role during mouse neutrophil clustering around particles of zymosan, a structural fungal component. Pioneer neutrophils recognizing zymosan or live *Candida albicans* displayed elevated calcium levels. Subsequently, a transient wave of calcium signals in neighboring cells was observed followed by the attraction of neutrophils that exhibited more persistent calcium signals as they reached zymosan particles. Calcium signals promoted LTB4 production while the blocking of extracellular calcium entry or LTB4 signaling abrogated cluster formation. Finally, using optogenetics to manipulate calcium influx in primary neutrophils, we show that calcium signals could initiate recruitment of neighboring neutrophils in an LTB4-dependent manner. Thus, sustained calcium responses at the center of the cluster are necessary and sufficient for the generation of chemoattractive gradients that attract neutrophils in a self-reinforcing process.

neutrophil | calcium | imaging | swarming | clustering

Neutrophils represent an essential and rapid line of defense against a variety of pathogens. One hallmark of neutrophils in vivo is their ability to form clusters or swarms in response to injury or infection (1–6). This phenomenon ensures the clearance of localized pathogens and promotes the sealing of tissue wounds but may also have deleterious effects such as alteration of lymph node architecture (1) or the formation of skin abscess (7). Such neutrophil collective behavior has been initially uncovered with the help of intravital imaging (1, 2, 4). Additionally, in vitro methods have been developed to study neutrophil clusters with high throughput (8). During neutrophil cluster formation, one or a few pioneer neutrophils (3) reach the site of damage/infection followed within minutes by the rapid and directional migration of many additional neutrophils toward the cluster (9). At later time points, neutrophil aggregation stops and mechanisms promoting cluster termination include chemoattractant receptor desensitization (10, 11) and factors secreted in the late phase of neutrophil aggregation such as LXA$_4$ (8). Central to this type of coordinated behavior is the ability of neutrophils to produce and respond to the same chemoattractants, forming the basis for a self-amplifying phenomenon (4, 8, 12). In a variety of settings, leukotriene B4 (LTB4) has been shown to be a major chemoattractant driving neutrophil cluster formation (4, 8, 9, 12).

Despite a detailed understanding of the spatiotemporal dynamics of neutrophil cluster formation, several key questions remain unanswered. Which signal drives pioneer neutrophil activity? In the context of sterile injury, cell death events have been shown to play an essential role in neutrophil swarming (4, 13). Whether neutrophil clusters during infection also primarily rely on cell death events or can be initiated by specific intracellular signaling events is unclear. Moreover, how neutrophils communicate in order to achieve spatially organized chemoattractant production remains to be fully understood. In an elegant study, Sarris and coworkers demonstrated that, in the context of sterile injury in zebrafish larvae, neutrophils communicate using adenosine triphosphate (ATP) through connexin hemichannels to generate calcium signals and produce LTB4 within the cluster (14). Whether calcium signals are also involved during mammalian neutrophil clustering and recognition of microbial products has not been investigated. It is also unclear whether calcium signals are sufficient to promote neutrophil clustering.

Here, we investigate the role of calcium signals in mouse neutrophil clusters formed during recognition of the fungal product, zymosan. Using in vitro and in vivo imaging, we show that zymosan recognition by pioneer neutrophils elicits a strong calcium response and transient calcium response in neighboring neutrophils that subsequently migrated directionally toward the cluster. Upon reaching zymosan particles, attracted neutrophils exhibited a sustained calcium elevation concomitant with their arrest.

Significance

During tissue damage or infection, neutrophils rapidly engage into a coordinated migration to form clusters. Neutrophil clustering is believed to contribute to wound sealing or pathogen clearance. Here we investigate the signals responsible for this collective behavior. We found that calcium signals in neutrophils recognizing microbial products promote the production of the neutrophil attractant LTB4, favoring the migration of additional neutrophils toward the cluster and additional calcium signals in a self-amplifying phenomenon.

We provide evidence that LTB4 production and calcium signaling were required for cluster amplification. Finally, by manipulating calcium signals using optogenetics, we show that calcium elevation is by itself sufficient to initiate some aspects of neutrophil clustering. Thus, spatially organized calcium signals orchestrate the self-amplifying neutrophil attraction that leads to cluster formation.

Results

Zymosan Induced Neutrophil Clusters In Vivo. To model neutrophil cluster formation upon recognition of microbial products, we used zymosan, a component of the fungal cell wall. Zymosan particles have been previously shown to trigger neutrophil clustering in vitro (8). To test whether zymosan could also induce neutrophil clusters in vivo, we injected fluorescent zymosan particles in the ear of LysM-eGFP mice (in which neutrophils express high levels of GFP) and performed intravital imaging. Neutrophils displayed strong accumulation and attraction toward the zymosan spot (Fig. 1A and B and Movie S1). Migrating neutrophils arrested when reaching the zymosan particles (Movie S1). In contrast, no clusters were detected in zymosan-free areas (Fig. 1A and B and Movie S1). Thus, zymosan effectively induced neutrophil clustering in vivo. Neutrophil swarms were not only detected in response to zymosan particles but were also detected following injection of live *Candida albicans* in vivo (Fig. 1C and Movie S2).

Calcium Signals during Neutrophil Cluster Formation In Vitro. Next, we thought to determine the initial signals triggering neutrophil cluster formation. Recognition of zymosan by neutrophils

or macrophages can induce Ca^{2+} influx (15, 16). When performing live imaging of neutrophil recognition of single zymosan particles in vitro, we observed that neutrophils increased intracellular calcium and arrested upon contact with zymosan (Fig. 2A and B and Movie S3). Additional calcium peaks were seen after the particles had been phagocytized (Movie S3). To investigate the spatiotemporal dynamics of calcium signals during neutrophil cluster formation, we imaged Indo1-loaded neutrophils in the presence of zymosan spots (containing 15 to 30 particles) as multiple zymosan particles are needed to elicit neutrophil clusters (8). We could identify several stages during neutrophil cluster formation (Fig. 2C and Movie S4). The first step consisted in one or a few neutrophils interacting with zymosan particles. These pioneer neutrophils exhibited strong calcium elevation and were completely arrested (Movie S4). Within a few minutes, a wave of transient calcium signal propagated from the nascent cluster to all neutrophils present within a radius of 100 to 150 μm from the center of the cluster (Fig. 2C and D and Movie S4). Upon rapid return of intracellular calcium concentration to basal levels, most neutrophils in this "alert" zone changed morphology, becoming more elongated and starting to migrate directionally toward the cluster (Fig. 2E–G and Movie S4). As these neutrophils were approaching the cluster, they exhibited sporadic calcium responses that became prolonged as they joined the pool of neutrophils contacting the zymosan particles (Fig. 2G–I and Movie S4). A collective and sustained calcium elevation at the center of the cluster was typically detected for the remaining duration of the movie (1 h). These results indicated that zymosan-induced neutrophil clusters are associated with robust calcium responses prominent at the center of the cluster and extending to more distant neutrophils (up to 100 to 150 μm away) in a more transient manner.
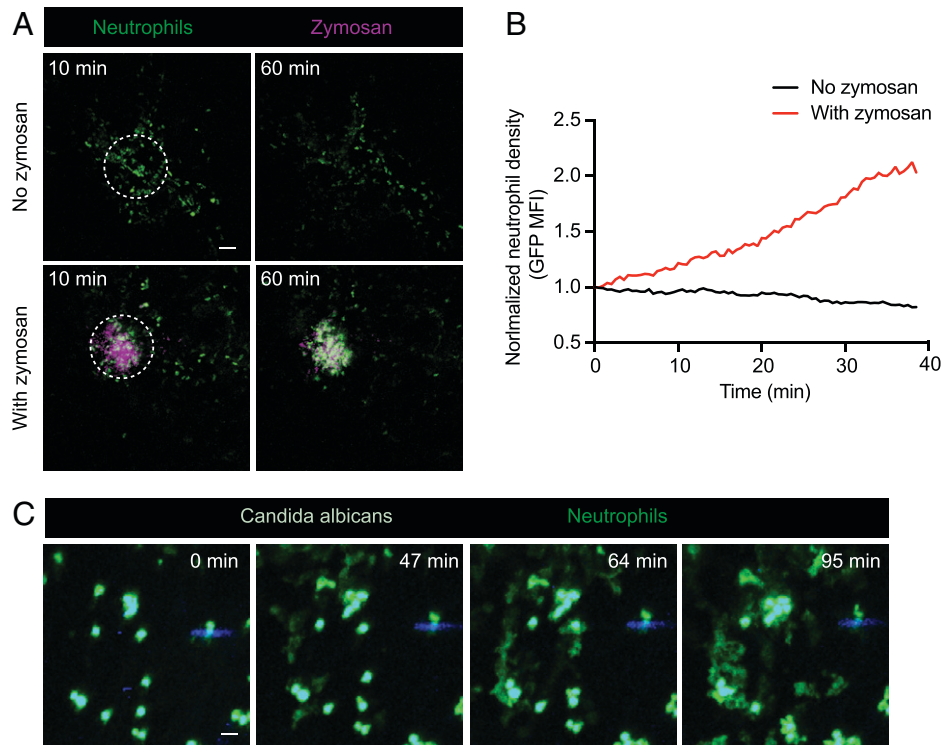

Fig. 1. Zymosan and live *C. albicans* trigger neutrophil cluster formation in vivo. LysM-eGFP mice were injected in the ear with zymosan particles and subjected to two-photon imaging for 1 h. (A) Representative time-lapse images showing that neutrophils (green) form a large cluster around zymosan particles (*Lower*) but do not cluster in area without zymosan (*Upper*). (B) Accumulation of neutrophils was quantified in the indicated regions (dashed circle) by measuring GFP fluorescence intensity over time. Values were normalized over the initial mean intensity measured at time 0. (Scale bar, 50 μm.) Data are representative of three independent experiments. (C) Neutrophil clustering in response to live *C. albicans*. LysM-eGFP mice were injected in the ear with live GFP-expressing *C. albicans* and subjected to two-photon imaging for up to 2 h. Representative time-lapse images show that neutrophils (green) form cellular clusters around *C. albicans*. Neutrophils and *C. albicans* both expressed GFP but were discriminated on the basis of their fluorescence intensity.
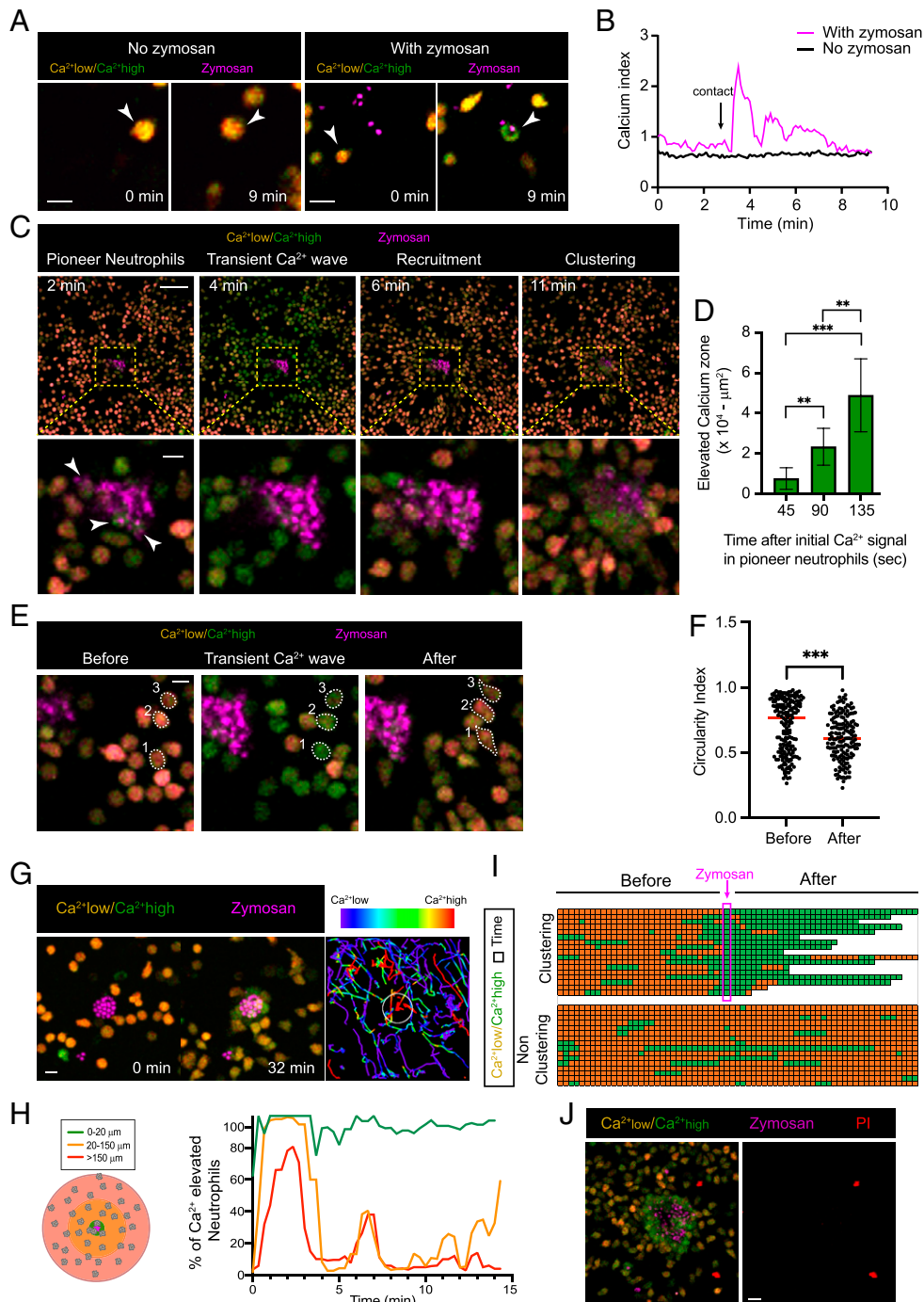
Fig. 2. Spatiotemporal dynamics of calcium signals during neutrophil clustering. Neutrophils were labeled with the calcium indicator Indo1 and cultured with zymosan particles. (*A*) Representative time-lapse images showing that recognition of zymosan particles by single neutrophils (white arrows) induces calcium signaling. (Scale bar, 10 μm.) Images are representative of three independent experiments. (*B*) Calcium index is graphed over time for an additional example of neutrophil contacting a zymosan particle and for a neutrophil that does not interact with zymosan. Black arrow on magenta curve indicates the time of contact between the neutrophil and the zymosan particle. (*C*) Calcium dynamics during neutrophil clustering proceed in different stages. Time-lapse images show different stages of neutrophil cluster formation over a spot of zymosan particles. Yellow dashed lines delineate zoomed-in areas shown in the *Lower* panel. (Scale bar [*Upper*], 50 μm; [*Lower*], 10 μm.) Data are representative of three independent experiments. (*D*) Propagation of a transient calcium wave from the center of the zymosan spot. The area showing neutrophils with elevated calcium is quantified at the indicated time points after the initial calcium response in pioneer neutrophils. Data are representative of three independent experiments. Bars show means ± SEM. Groups were compared using a two-tailed unpaired *t* test, ***$P < 0.001$, **$P < 0.01$. (*E*) Time lapse images showing the morphological changes in neutrophil shape after the transient calcium wave. White dashed lines highlight neutrophil cell shape. (*F*) Quantification of the cell sphericity index during and after the transient calcium wave. A circular shape corresponds to an index of 1. Each dot represents one neutrophil. Only cells exhibiting a calcium response were analyzed. Bars represent mean values. Statistical significance was assessed using a two-tailed unpaired *t* test, ***$P < 0.001$. (*G*) Representative tracks of neutrophils migrating toward a zymosan spot. Each line corresponds to a neutrophil trajectory. Tracks are color coded with calcium levels, showing calcium elevation in approaching neutrophils. The white circle delineates the zymosan spot. (*H*) Percentage of neutrophils with elevated calcium content was measured at different distances from the center of zymosan particles and plotted over time. (*I*) Figure compiles calcium signals in representative neutrophils before and after reaching the zymosan spot (*Upper*). Each line represents one neutrophil followed over time. Data are aligned to the time of zymosan recognition. Colored squares show the time points during which the neutrophil is visible within the imaging field. Orange and green indicate the time period during which the calcium level in neutrophil is low or high, respectively. The magenta box indicates the initial time point at which neutrophils reach the zymosan spot. *Lower* panel shows representative neutrophils that did not participate in the cluster. Data are representative of at least five independent experiments. (*J*) Neutrophil clustering was imaged in the presence of propidium iodide (red) to detect dead cells. (Scale bar, 10 μm.) Results are representative of three independent experiments.

Notably, neutrophil recognition of live *C. albicans* also resulted in calcium responses associated with cluster formation (*SI Appendix*, Fig. S1 and Movie S5). Since loss of membrane integrity can lead to intracellular calcium elevation, we tested whether some of the detected calcium signals were due to cell death events. However, repeating these experiments in the presence of propidium iodide did not support a major role for cell death in the signals detected (Fig. 2*J* and Movie S6).

To test the importance of calcium influx in the process of neutrophil clustering, we analyzed neutrophils in the presence of zymosan and ethylene glycol tetraacetic acid (EGTA) in order to chelate extracellular calcium. Neutrophil cluster formation was abrogated in the absence of extracellular calcium, suggesting that calcium influx is required for the coordinated neutrophil clustering (Fig. 3 and Movie S7). We also tested the impact of calcium chelation at later time point when the cluster had already started to form. As shown in Movie S8, addition of EGTA rapidly arrested ongoing neutrophil cluster formation. It remains formally possible that calcium chelation affects other aspects of neutrophil biology such as adhesion properties that could potentially limit cluster formation. However, blocking CD18 did not prevent cluster formation around zymosan particles (*SI Appendix*, Fig. S2). Our results supported the idea that calcium signals play a major role during neutrophil cluster formation in these in vitro settings.

Robust Calcium Signaling during Neutrophil Clustering In Vivo.

To test whether calcium signals are also associated with cluster formation in vivo, we generated bone marrow chimeras by reconstitution of irradiated mice with hematopoietic stem cells (HSCs) retrovirally transduced to express the genetically encoded calcium reporter, Twitch2B (17) (Fig. 4*A* and *B*). Chimeric mice were injected with zymosan particles in the ear dermis and immediately subjected to intravital imaging. As expected, cells with the typical morphology and migratory behavior of neutrophils rapidly accumulated around the zymosan spot once pioneer cells reached the zymosan particles (Fig. 4*C* and *D* and Movie S9). Clusters were not detected in areas without zymosan (Fig. 4*C*). Most importantly, we observed strong and prolonged calcium elevation in neutrophils contacting the zymosan, while approaching neutrophils exhibited transient calcium responses (Movie S9). Thus, neutrophil cluster formation is also associated with strong calcium signaling in vivo.

Reciprocal Amplification of Calcium Signals and LTB4 Production Participate in Neutrophil Clustering.

We next asked how calcium signals at sites of zymosan recognition may contribute to cluster formation. The lipid mediator LTB4 is well known to participate in neutrophil swarming in response to sterile injury or pathogens. Zymosan recognition by neutrophils induced LTB4 production that was largely dependent on extracellular calcium (Fig. 5*A* and *B*). Moreover, eliciting a calcium influx in neutrophils using thapsigargin directly triggered LTB4 production (Fig. 5*A* and *B*). Reciprocally, neutrophils exhibited increased intracellular calcium concentration in response to LTB4 (Fig. 5*C*). Moreover, antagonizing LTB4 receptors largely reduced neutrophil clustering around zymosan particles (Fig. 5*D* and *E* and Movie S10). In these settings, the early calcium wave was reduced and subsequent calcium signals were only detected in neutrophils initially contacting the zymosan particles (Movie S10). No attraction of remote neutrophils was observed. To confirm the importance of LTB4 in our settings, we used MK886 an inhibitor of arachidonate 5-lipoxygenase (Alox5), an essential enzyme for LTB4 synthesis. As shown in Fig. 5*F* and *G*, neutrophils strongly reduced cluster formation around zymosan in the presence of MK886. We also tested the role of connexin hemichannels as well as ATP production since they play an important role in neutrophil swarming in the zebrafish model of sterile injury. Cluster formation was not affected in the presence of NF279, an antagonist of P2X receptors (Fig. 5*F* and *G*). In the presence of carbenoxole (CBX), an inhibitor of gap junctions, neutrophils also continued to form large clusters around zymosan particles with a modest reduction in cluster size that did not reach statistical significance (Fig. 5*F* and *G*). This suggests that propagation of calcium signals through ATP and connexins is dispensable for neutrophil clustering triggered by zymosan recognition.

Our results support a model in which zymosan recognition directly triggers calcium elevation and LTB4 production, attracting more neutrophils that engage in LTB4 production as they approach and reach the zymosan spot (responding to local LTB4 concentration and zymosan particles).

Optogenetic Manipulation of Calcium Signals in Neutrophils Supports a Causative Role for Calcium in Cluster Formation.

Our results and that of a recent study (14) support a role for calcium signals during neutrophil clustering in mouse and zebrafish, respectively. However, it is unclear whether calcium signals are by themselves sufficient to initiate some aspects of neutrophil clustering. To address this issue, we relied on
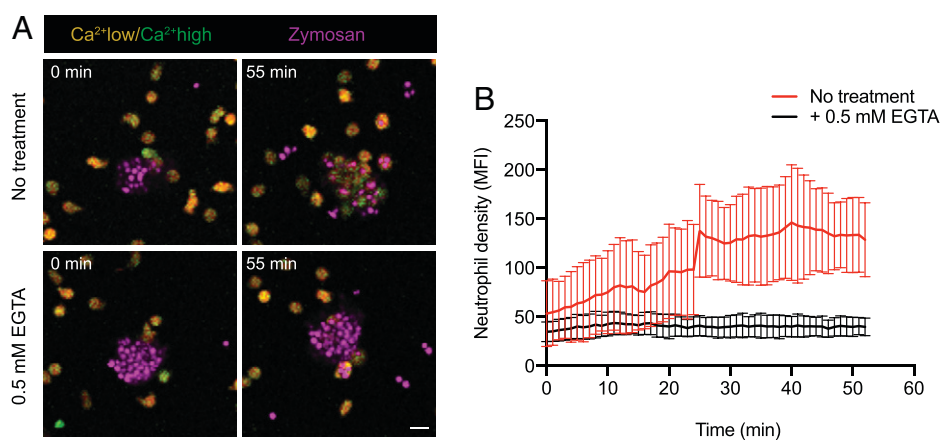
Fig. 3. The formation of neutrophil clusters around zymosan particles requires extracellular calcium. (*A*) Representative time-lapse images of Indo1-labeled neutrophils cluster formation around the zymosan spot in the presence (*Lower*) or absence (*Upper*) of 0.5 mM EGTA. (Scale bar, 10 μm.) (*B*) Quantification of neutrophil density over time in the presence (black) or absence (red) of 0.5 mM EGTA. Data are pooled from three independent experiments.
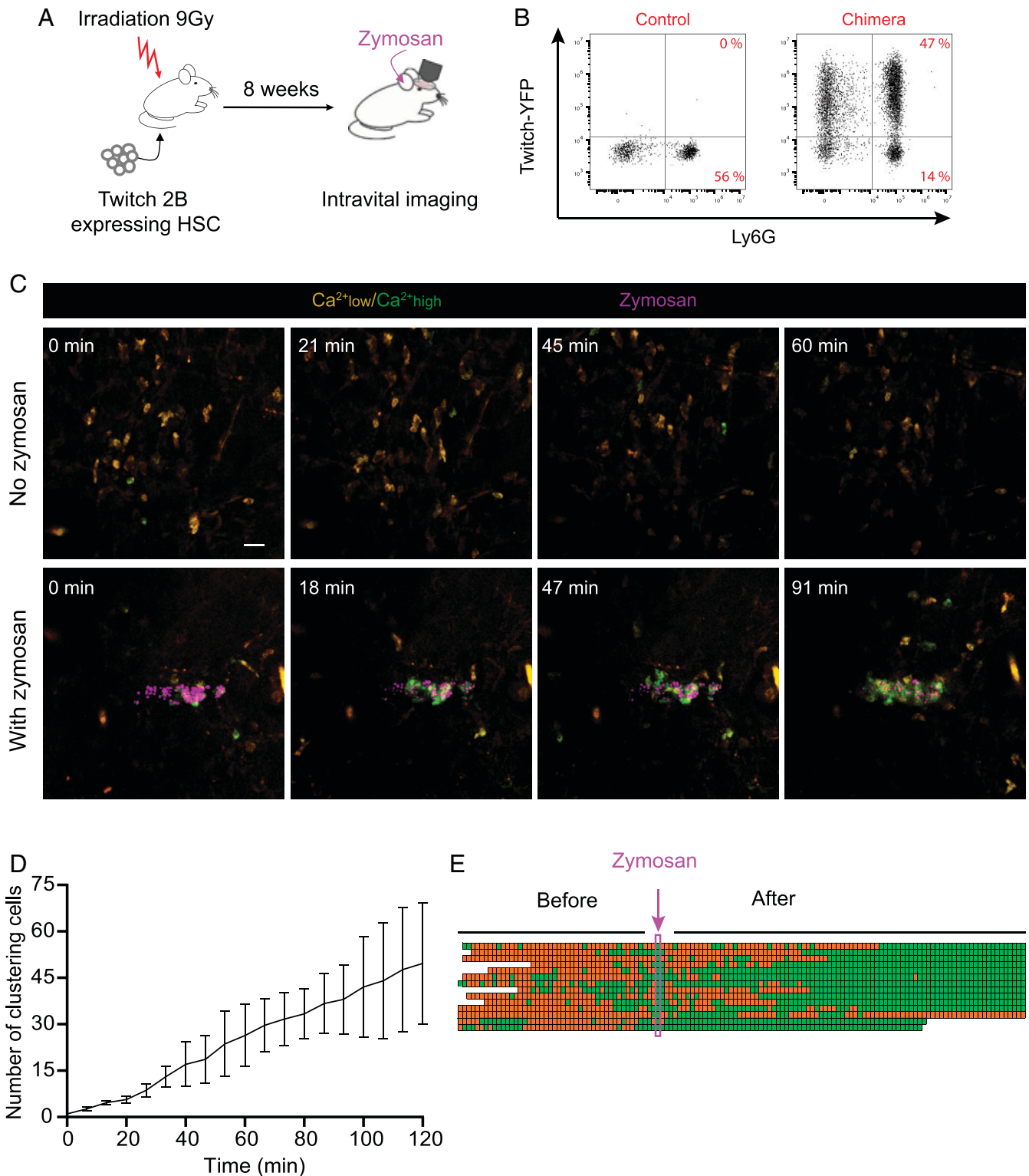
Fig. 4. Robust calcium signals during neutrophil clustering in vivo. (*A*) Experimental set-up. Chimeric mice were reconstituted with HSCs expressing the FRET-based calcium indicator Twitch2B. Eight weeks later, mice were injected with zymosan particles in the ear and subjected to intravital imaging. (*B*) Flow cytometry dot plots showing the reconstitution of chimeric mice and percentage of neutrophils expressing Twitch2B. (*C*) Time-lapse images showing calcium levels (as measured by FRET signals with Twitch2B) in neutrophils in the presence (*Lower*) or absence (*Upper*) of a zymosan spot (magenta). (Scale bar, 50 μm.) (*D*) Quantification of absolute number of neutrophils clustering at the zymosan spot during 2 h of imaging. Data are pooled from two independent experiments. (*E*) Figure compiles calcium signals in several neutrophils before and after reaching the zymosan spot. Each line represents one neutrophil followed over time. Data are aligned to the time of zymosan recognition. Colored squares show the time points during which the neutrophil is visible within the imaging field. Orange and green indicate the time period during which the calcium level in neutrophil is low or high, respectively. The magenta box indicates the initial time point at which neutrophils reach the zymosan spot. Data are representative of three independent experiments.
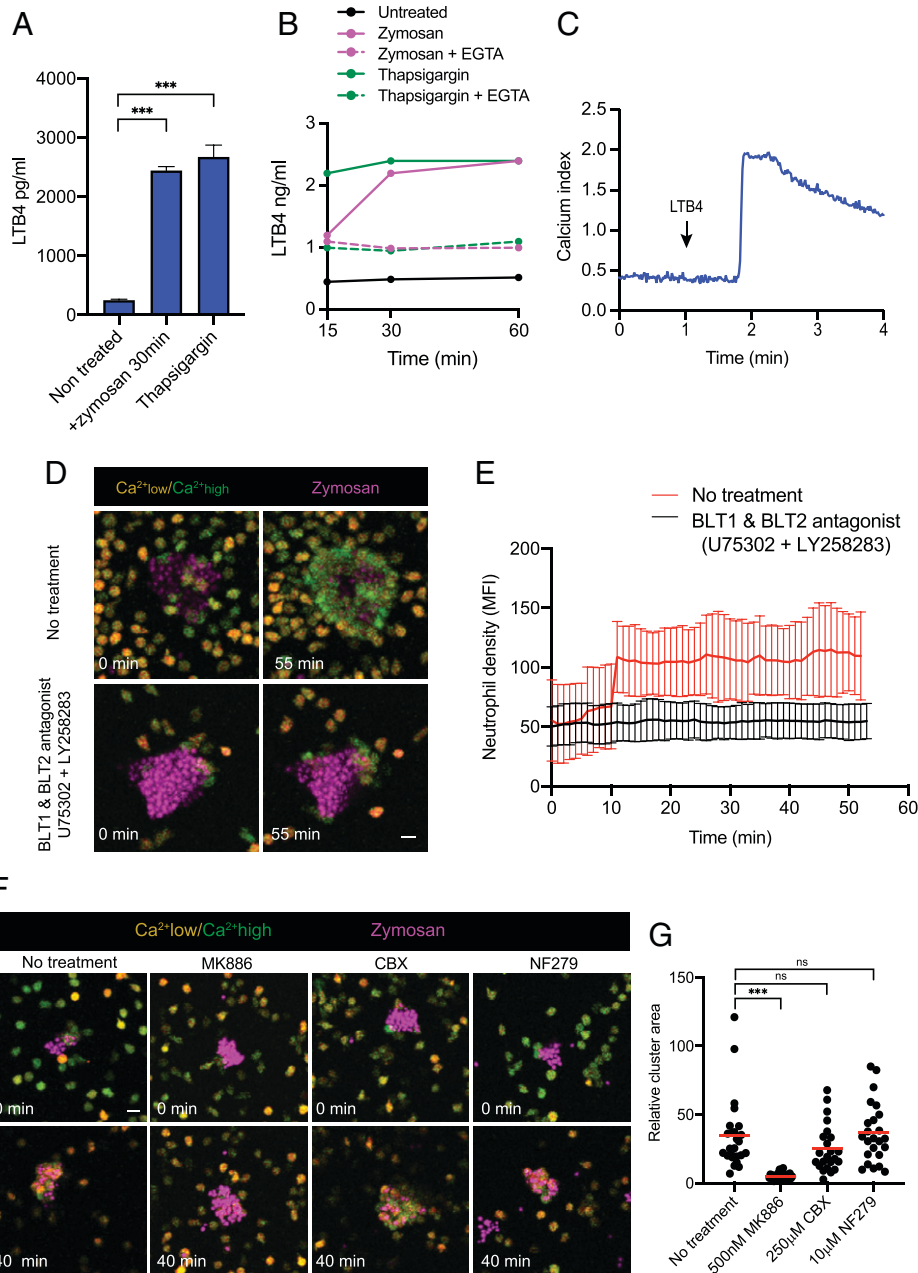
Fig. 5. Calcium signals and LTB4 production participate jointly in neutrophil cluster formation and expansion. (*A*) Neutrophils secrete LTB4 in the presence of zymosan particles or upon treatment with thapsigargin. Statistical significance was assessed using two-tailed unpaired *t* test. ***$P < 0.001$. (*B*) LTB4 production by neutrophils in response to zymosan in the presence or absence of EGTA. (*C*) Intracellular calcium elevation in Indo1-labeled neutrophils treated with 50 ng/mL of LTB4 using time-resolved flow cytometry. Calcium responses are shown as averaged kinetic curves. (*D*) Time-lapse images of Indo1-labeled neutrophils around a zymosan spot (magenta) in the presence or absence of 20 μM U75302 and 20 μM LY255283 (BLT1 and BLT2 antagonists, respectively). (Scale bar, 10 μm.) Data are pooled from three independent experiments. (*E*) Quantification of neutrophil density over time in the presence (black) or absence of 20 μM U75302 and 20 μM LY255283 (red). (*F* and *G*) Neutrophil cluster formation was evaluated in the presence of inhibitor of LTB4 synthesis MK886, the inhibitor of gap junction CBX, or the antagonist of P2X receptors NF279. (*F*) Representative time-lapse images depicting neutrophil clustering in the presence or absence of the indicated drug. (*G*) Quantification of neutrophil cluster size around zymosan particles normalized to number of zymosan particles per spot. Statistical significance was assessed using two-tailed unpaired *t* test. ***$P < 0.001$; ns, not significant.

optogenetics to directly manipulate neutrophils with light. We used the eOS1 actuator, an improved version of OptoSTIM1, that relies on Cry2-mediated clustering of STIM-1 upon light exposure to trigger calcium release–activated calcium (CRAC) channel opening and extracellular calcium influx (18). To introduce the actuator in primary neutrophils, we generated bone marrow chimeras by retroviral transduction of eOS1 in HSCs (Fig. 6*A* and *B*). After reconstitution, neutrophils were purified from chimeric mice. We confirmed that eOS1-positive but not eOS1-negative neutrophils exhibited intracellular calcium elevation upon blue light illumination as detected by flow

cytometry (Fig. 6*C*). Using live imaging, we also photoactivated a mixture of neutrophils from eOS1 chimeras and control mice. As shown in Fig. 6*D*, only eOS1-positive but not control neutrophils responded to a short light pulse. To test whether calcium influx in individual neutrophils may recapitulate some aspects of neutrophil clustering, we illuminated neutrophils from the chimeric mice (containing ~30% of eOS1-positive neutrophils). We observed that after photoactivation, isolated responding neutrophils could promote the attraction and calcium responses of neighboring neutrophils (Fig. 6*E* and Movie S11), whereas no clusters were induced when control neutrophils (that
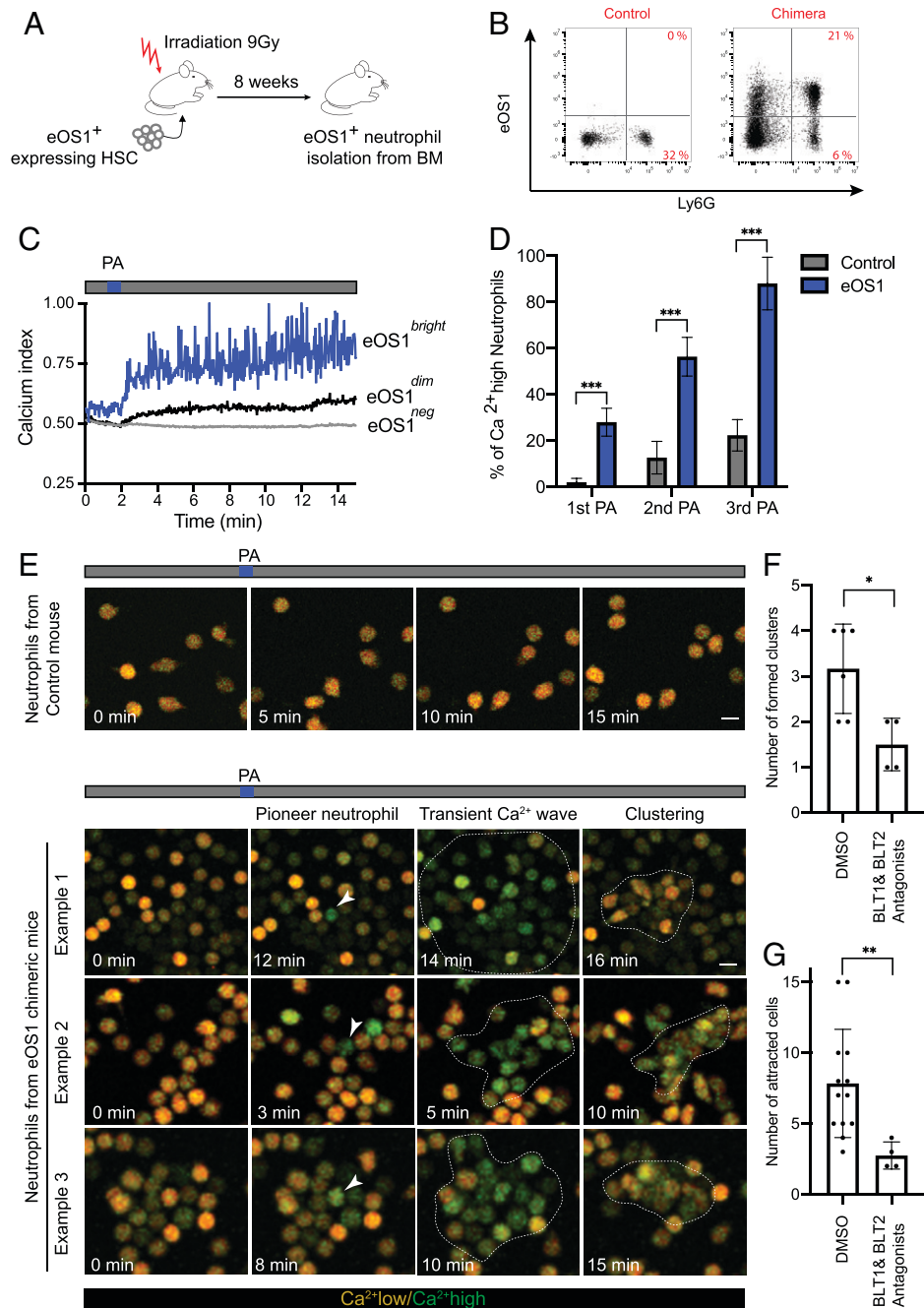
Fig. 6. Optogenetic manipulation of calcium signals in neutrophils supports a causative role for calcium in cluster formation. (*A*) Experimental set-up. Chimeric mice were reconstituted with HSCs expressing the calcium actuator eOS1. After 8 wk, eOS1-expressing neutrophils were isolated from the chimeras. (*B*) Flow cytometry dot plots showing the reconstitution of chimeric mice and percentage of neutrophils expressing eOS1. (*C*) Neutrophils isolated from the chimeric mice were loaded with the Indo1 calcium indicator. Cells were subjected to time-resolved flow cytometry and illuminated with an external LED (470 nm) during the acquisition at the indicated time point. Calcium responses shown as averaged kinetic curves of neutrophils expressing different levels of eOS1 plasmid (bright, dim, or neg). PA indicates the timing of photoactivation during the experiment. Data are representative of four independent experiments. (*D*) A mixture (1:1 ratio) of neutrophils isolated from eOS1[+] chimeric mice (uncolored) and neutrophils isolated from wild-type mice (loaded with SNARF) was prepared. Cells were loaded with Indo1 and subjected to live imaging. Photoactivation was induced using LED (470 nm) every 10 min for 10 s. Percentages of responding cells are shown upon each PA cycle. (*E*) Time-lapse images depicting neutrophils and calcium dynamics upon photoactivation. Arrowheads show the initial neutrophils responding to photoactivation. Dashed lines in the third and fourth panels highlight the transient Ca^{2+} wave and the formation of a neutrophil cluster, respectively. (Scale bar, 10 μm.) Data are representative of four independent experiments. (*F* and *G*) The number of formed clusters in the field of view (*F*) and the total number of attracted cells per cluster (*G*) was quantified after PA of eOS1-expressing neutrophils in the presence or absence of BLT1 and BLT2 antagonists. Data are pooled from three independent experiments. Bars show means ± SEM. Groups were compared using a two-tailed unpaired *t* test, ***$P < 0.001$, **$P < 0.01$, *$P < 0.1$.

did not express eOS1) were photoactivated (Fig. 6*E*). Of note, only small clusters were formed, possibly because additional factors (not associated with calcium signals) were missing or because only isolated cells were stimulated (as opposed to multiple cells in a zymosan spot). To confirm that neutrophil aggregates generated by optogenetic manipulation of calcium signals also shared the requirement for LTB4 signaling,

we performed photoactivation in the presence of BLT1/BLT2 antagonists. As shown in Fig. 6*F* and *G*, both the number of clusters formed and the size of the clusters were substantially reduced when interfering with LTB4 signaling. In summary, our optogenetic manipulation strongly suggested that calcium signals make a causative contribution to LTB4-dependent neutrophil cluster formation.

Discussion

We characterized here the spatiotemporal dynamics of calcium signals during neutrophil clustering (or swarming) around the fungal component zymosan in vitro and in vivo. Calcium signals appeared spatially organized, being prominent at the cluster center and essential to promote the self-amplification phenomenon mediated in part through LTB4 production and signaling. In a model of sterile injury in the zebrafish, neutrophils were recently shown to exhibit strong intracluster calcium responses, favored by the recognition of necrotic tissue and intercellular neutrophil communication through ATP and connexin-43 hemichannels (14). In our settings, direct recognition of zymosan particles appears sufficient to elicit calcium signals in neutrophils. This is consistent with the fact that zymosan recognition by Dectin-1 triggers a calcium flux in neutrophils that is dependent on Stim1 and Stim2 (16). Such strong signaling events may also bypass the need for cell death of pioneer neutrophils to initiate clustering as seen in models of tissue damage (19, 20). Thus, while signals triggering calcium elevation may vary in distinct contexts and likely coexist, an intense calcium response at the cluster center may represent a general feature of LTB4-mediated neutrophil attraction. Moreover, such a local chemoattractant production is further favored by the fact that intracellular calcium elevation promotes cell arrest (21–23) and hence cell accumulation over time. Calcium signals were both necessary and to some extent sufficient for cluster formation. Yet, it was notable that optogenetic manipulation in isolated neutrophils leads to the formation of clusters of small sizes, in line with the proposed idea that a quorum sensing mechanism controls neutrophil cluster formation (24). Future in vivo application of optogenetics in neutrophils may help understand how the number of stimulated neutrophils controls the size and duration of cellular clusters and whether forcing neutrophil clustering may have beneficial consequences in the context of infection or cancer. In sum, neutrophils can use recognition of microbial products and calcium signals to amplify their own recruitment in a spatially organized manner. Uncovering the tissue distribution of chemoattractants over time remains a challenging goal but could provide additional key insights into the complex process of neutrophil clustering in vivo.

Materials and Methods

Mice. Six- to eight-week-old C57BL/6J mice were purchased from ENVIGO. LysM-eGFP mice were bred in our animal facility under specific pathogen-free conditions. We used age- and sex-matched mice for all experiments. All animal studies were approved by the Institut Pasteur Safety Committee in accordance with French and European guidelines (CETEA 190148).

Neutrophil Isolation. Femurs and tibias were isolated from adult wild-type (WT) or chimeric mice, sterilized in 70% ethanol, and flushed with phosphate-buffered saline (PBS). Single-cell suspensions were prepared by filtering the marrow through a 70-μm cell strainer. Neutrophils were sorted by negative selection using a mouse isolation kit following manufacture instructions (Miltenyi). Cells were then cultured in complete RPMI medium 1640 (supplemented with 10% heat-inactivated fetal bovine serum, 100 U/mL penicillin, 100 ng/mL streptomycin, 1 mM sodium pyruvate, 10 mM Hepes, and 5 μM 2-mercaptoethanol) and used within 24 h.

In Vitro Imaging of Neutrophil Cluster Formation. Plastic dishes were coated with poly-D-lysine (Sigma, 0.01% dilution in H_2O) for 10 min at 37 °C and washed with PBS before loading cells. Neutrophils were stained with Indo1/AM (2.5 μM, Molecular Probes) for 40 min at 37 °C. Labeled neutrophils were washed and resuspended in complete RPMI without phenol red. Cluster formation was initiated by gently transferring labeled neutrophils in plastic dishes and adding zymosan particles (Thermo Fisher) at the beginning of the recording. Alternatively, zymosan particles or live GFP-expressing *C. albicans* were precoated on glass dishes using micropatterning stamps (4Dcell) following manufacturer's instructions. The fluorescent strain of *C. albicans* (CEC4950) is a derivative of the reference strain SC5314, in which the GFP placed under the control of the strong constitutive promoter P_{TDH3} was integrated at the $RPS1$ locus. Imaging was performed using a two-photon microscope. Excitation was provided by an InSight DeepSee dual laser (Spectra-Physics) tuned at 720 nm (for Indo1, zymosan, and propidium iodide [PI] imaging), 880 nm for GFP and 1,040 nm (for Seminaphtharhodafluor [SNARF] imaging). The following filter sets were used: Indo1: 483/32 and 390/40, PI: 624/40, zymosan-Alexa594: 593/35, SNARF: 607/70, GFP: 512/25. Temperature was maintained at 37 °C with a heating ring. Ca^{2+} signals were quantified using the ratio of calcium-bound to calcium-free fluorescence as described previously (18). Images were analyzed using Fiji software. Cluster formation was evaluated by measuring neutrophil density around the zymosan spot over time. For optogenetic experiments, eOS1-expressing or control neutrophils were placed in a poly-D-lysine–coated plate and photoactivated using a 470-nm blue light LED (Leica) for 15 s. Image acquisition was performed as described above. When indicated, control neutrophils were labeled with SNARF. For inhibition of BLT1 and BLT2, we used LY255283 and U75302 (dissolved in ethanol at 1 mM, Abcam). Both compounds were added to the culture media at a concentration of 20 μM. Neutrophils were left in the incubator for 15 min before addition to the zymosan-coated plastic dishes. For testing the effect of EGTA on neutrophil migration during clustering, neutrophils were resuspended in culture media containing 0.5 μM EGTA. Alternatively, EGTA was added at the same concentration 5 min after neutrophil cluster formation was detected.

Generation of Bone Marrow Chimeric Mice. Bone marrow cells were isolated from femurs and tibias of C57BL/6J adult mice by flushing bone marrow with PBS. Red blood cells were removed through Ficoll-Paque separation (GE Healthcare). Cells were then washed and resuspended in complete media supplemented with 100 ng of mouse stem cell factor (m-SCF), 20 ng of m-IL-3 and 20 ng of m- IL-6 (Peprotech) and incubated over night at 37 °C. These cells were retrovirally transduced to express either the fluorescence resonance energy transfer (FRET)-based Twitch2B calcium indicator (17) or calcium actuator mScarlet-OptoSTIM-1 (eOS1) (18). Wild-type C57BL/6J recipient mice were γ-irradiated with a single dose of 9 Gy. Four hours later, irradiated mice were reconstituted with a total of 4×10^6 transduced bone marrow cells via intravenous (i.v.) injection. Mice were used 6 to 12 wk after reconstitution. Reconstitution was confirmed by flow cytometry by staining blood cells with a Alexa647-conjugated anti-Ly6G-mAb (clone 1A8, BD).

Intravital Imaging. Mice were anesthetized with a mixture of xylazine (Rompun, 10 mg/kg) and ketamine (Imalgene, 100 mg/kg), which was replenished hourly. Zymosan-Alexa594 particles or live GFP-expressing *C. albicans* (2×10^4) were diluted in 50 μL PBS and 5 μL was injected in the ear of the indicated recipients (5). Intravital imaging was performed 15 min after injection. Two-photon imaging was performed with an upright microscope FVMPE-RS (Olympus) and a 25×/1.05 numerical aperture (N.A.) water-dipping objective (Olympus). Excitation was provided by an InSight DeepSee dual laser (Spectra Physics) tuned at 880 nm. The following filter sets were used for imaging: Twitch2B (CFP: 483/32 and YFP: 542/27), zymosan-Alexa594 (593/35), GFP (512/25). A 25-μm-thick volume of tissue was scanned at 5-μm Z steps and 10- to 30-s intervals. Images were processed and analyzed using Fiji software. Movies and figures based on two-photon microscopy are shown as two-dimensional maximum intensity projections of three-dimensional data.

Calcium Measurement by Flow Cytometry. Neutrophils isolated from either C57BL/6J mice or chimeric mice expressing mScarlet-eOS1actuator were stained with Indo1/AM (2.5 μM, Molecular Probes) for 40 min at 37 °C. Cells were washed and kept at 37 °C in complete medium at a concentration of 10^6 cells/mL. Calcium measurements were performed on a CytoFLEX LX cytometer (Beckman Coulter) using CytExpert 2.3 software (Beckman Coulter). A baseline Indo1 fluorescence was recorded for 1 to 2 min; cells were then photoactivated by placing a LED (470 nm, 710 mW, THORLabs) in front of the fluorescence activated cell sorting (FACS) tube for 60 s at the indicated time point while cell acquisition continued. A calcium index was calculated as the ratio of the fluorescent

signals at 405 nm (Ca^{2+} bound dye, 405/30 BP) to that at 485 nm (Ca^{2+} free dye, 525/40 BP) and followed over time. A kinetic analysis was performed with FlowJo software version 10.4 (Tree Star) and the smoothed geometric means of Indo1 ratio were plotted.

Measurement of LTB4 Production. Neutrophils were resuspended in complete RPMI either untreated or stimulated with 2×10^4 zymosan particles for 15 and 30 min. Alternatively, neutrophils were stimulated with a mixture of phorbol myristate acetate (PMA) (100 ng/mL) and ionomycin (1 μg/mL) or thapsigargin (1 μM) for 30 min (all purchased from Sigma). Supernatants were recovered and the secretion of LTB4 was measured using a LTB4 parameter assay kit (R&D Systems).

1. T. Chtanova *et al.*, Dynamics of neutrophil migration in lymph nodes during infection. *Immunity* **29**, 487–496 (2008).
2. B. McDonald *et al.*, Intravascular danger signals guide neutrophils to sites of sterile inflammation. *Science* **330**, 362–366 (2010).
3. L. G. Ng *et al.*, Visualizing the neutrophil response to sterile tissue injury in mouse dermis reveals a three-phase cascade of events. *J. Invest. Dermatol.* **131**, 2058–2068 (2011).
4. T. Lämmermann *et al.*, Neutrophil swarms require LTB4 and integrins at sites of cell death in vivo. *Nature* **498**, 371–375 (2013).
5. J. L. Li *et al.*, Intravital multiphoton imaging of immune responses in the mouse ear skin. *Nat. Protoc.* **7**, 221–234 (2012).
6. Q. Deng *et al.*, Localized bacterial infection induces systemic activation of neutrophils through Cxcr2 signaling in zebrafish. *J. Leukoc. Biol.* **93**, 761–769 (2013).
7. J. Liese, S. H. Rooijakkers, J. A. van Strijp, R. P. Novick, M. L. Dustin, Intravital two-photon microscopy of host-pathogen interactions in a mouse model of *Staphylococcus aureus* skin abscess formation. *Cell. Microbiol.* **15**, 891–909 (2013).
8. E. Reátegui *et al.*, Microscale arrays for the profiling of start and stop signals coordinating human-neutrophil swarming. *Nat. Biomed. Eng.* **1**, 0094 (2017).
9. K. Kienle, T. Lämmermann, Neutrophil swarming: An essential process of the neutrophil tissue response. *Immunol. Rev.* **273**, 76–93 (2016).
10. C. Coombs *et al.*, Chemokine receptor trafficking coordinates neutrophil clustering and dispersal at wounds in zebrafish. *Nat. Commun.* **10**, 5166 (2019).
11. K. Kienle *et al.*, Neutrophils self-limit swarming to contain bacterial growth in vivo. *Science* **372**, eabe7729 (2021).
12. T. Németh, A. Mócsai, Feedback amplification of neutrophil function. *Trends Immunol.* **37**, 412–424 (2016).
13. P. Sagoo *et al.*, In vivo imaging of inflammasome activation reveals a subcapsular macrophage burst response that mobilizes innate and adaptive immunity. *Nat. Med.* **22**, 64–71 (2016).
14. H. Poplimont *et al.*, Neutrophil swarming in damaged tissue is orchestrated by connexins and cooperative calcium alarm signals. *Curr. Biol.* **30**, 2761–2776.e7 (2020).
15. M. Girotti, J. H. Evans, D. Burke, C. C. Leslie, Cytosolic phospholipase A2 translocates to forming phagosomes during phagocytosis of zymosan in macrophages. *J. Biol. Chem.* **279**, 19113–19121 (2004).
16. R. A. Clemens, J. Chong, D. Grimes, Y. Hu, C. A. Lowell, STIM1 and STIM2 cooperatively regulate mouse neutrophil store-operated calcium entry and cytokine production. *Blood* **130**, 1565–1577 (2017).
17. T. Thestrup *et al.*, Optimized ratiometric calcium sensors for functional in vivo imaging of neurons and T lymphocytes. *Nat. Methods* **11**, 175–182 (2014).
18. A. Bohineust, Z. Garcia, B. Corre, F. Lemaître, P. Bousso, Optogenetic manipulation of calcium signals in single T cells in vivo. *Nat. Commun.* **11**, 1143 (2020).
19. H. M. Isles *et al.*, Pioneer neutrophils release chromatin within in vivo swarms. *eLife* **10**, e68755 (2021).
20. K. M. Glaser, K. Mihlan, T. Lämmermann, Positive feedback amplification in swarming immune cell populations. *Curr. Opin. Cell Biol.* **72**, 156–162 (2021).
21. P. A. Negulescu, T. B. Krasieva, A. Khan, H. H. Kerschbaum, M. D. Cahalan, Polarity of T cell shape, motility, and sensitivity to antigen. *Immunity* **4**, 421–430 (1996).
22. E. Donnadieu, G. Bismuth, A. Trautmann, Antigen recognition by helper T cells elicits a sequence of distinct changes of their shape and intracellular calcium. *Curr. Biol.* **4**, 584–595 (1994).
23. N. R. Bhakta, D. Y. Oh, R. S. Lewis, Calcium oscillations regulate thymocyte motility during positive selection in the three-dimensional thymic environment. *Nat. Immunol.* **6**, 143–151 (2005).
24. M. Palomino-Segura, A. Hidalgo, Immunity: Neutrophil quorum at the wound. *Curr. Biol.* **30**, R828–R830 (2020).